Filament stretching and capillary breakup extensional rheometry measurements of viscoelastic wormlike micelle solutions

Avinash Bhardwaj, Erik Miller, and Jonathan P. Rothstein[a)]

Department of Mechanical and Industrial Engineering, University of Massachusetts, Amherst, Massachusetts 01003

(Received 11 August 2006; final revision received 20 February 2007)

Synopsis

A filament stretching extensional rheometer and capillary breakup extensional rheometer are used to measure the extensional rheology of a series of wormlike micelle solutions experiencing a uniaxial elongational flow. The experiments are performed using a series of wormlike micelle solutions of both cetylpyridinium chloride and sodium salicylate (NaSal) in an aqueous sodium chloride solution and cetyltrimethylammonium bromide and NaSal in de-ionized water. The linear viscoelasticity of all the wormlike micelle solutions is well described by a Maxwell model with just one or two relaxation times while the steady shear measurements all demonstrate characteristics of shear banding at large shear rates. In transient homogeneous uniaxial extension imposed by a filament stretching rheometer, each of the wormlike micelle solutions demonstrate significant strain hardening. At large extension rates, the wormlike micelle solution filaments are all found to fail through a dramatic rupture near the axial midplane at a constant stress independent of imposed extension rate. The result is an extensional viscosity that decays linearly with increasing extension rate. This filament failure likely stems from the local scission of individual wormlike micelle chains. For the more concentrated solutions, as the imposed extension rate is reduced, a critical extension rate is found below which the filament does not rupture, but instead elastocapillary pinch off is recovered and the elastic tensile stresses achieved in the fluid filament grow far beyond the value observed at rupture. This dramatic upturn in the elastic tensile stress and the extensional viscosity at low extension rates is not intuitively expected and is most likely a result of structural changes to the entangled wormlike micelle solution. Strain hardening is also observed in capillary breakup rheometry experiments, however, when the results of filament stretching and capillary breakup rheometry measurements at nominally the same extension rate are superimposed, the results do not agree; the extensional viscosity measurements from filament stretching are in some instances more than an order of magnitude larger. This result calls into question the use of capillary breakup rheometry for quantitatively measuring the extensional viscosity of wormlike micelle solutions. © *2007 The Society of Rheology.*
[DOI: 10.1122/1.2718974]

I. INTRODUCTION

Surfactants are molecules that consist of a hydrophilic head group and a hydrophobic tail. When dissolved in water they can spontaneously form several different types of self-assembling aggregates [Israelachvili (1985); Larson (1999); Rehage and Hoffmann

[a)]Author to whom correspondence should be addressed; electronic mail: rothstein@ecs.umass.edu

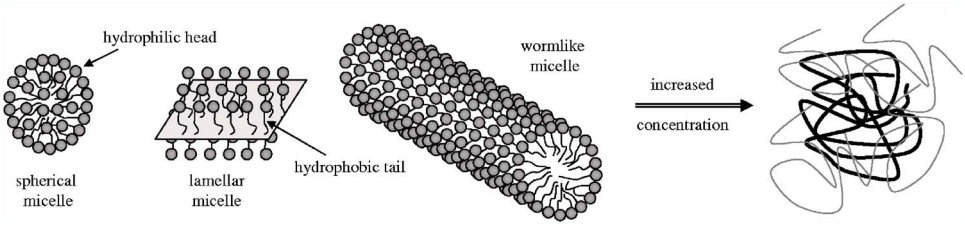

FIG. 1. Schematic diagram of wormlike micelle solutions showing various morphologies including spherical, lamellar, wormlike and long entangled wormlike micelles that can impart viscoelasticity.

(1991)]. As seen in Fig. 1, the size and shape of the resulting aggregate morphology can range from spherical micelles, to wormlike micelles to lamellae depending on surfactant and counterion concentration and interaction [Lequeux and Candau (1997)]. An enormous amount of research has been devoted to investigating the morphology, phase transitions, and the shear and extensional rheology of different surfactant solutions [Cates (1987); Olmsted (1999); Rehage and Hoffmann (1991); Rothstein (2003); Shikata and Kotaka (1991); van Egmond (1998)]. Under the proper conditions, the micelles, resembling slender rods, can entangle and impart viscoelasticity to the fluid [Cates (1987)]. The difference between these wormlike micelles and polymers is that the micelles continuously break and reform with time. This leads to a broad and dynamic distribution of micelle lengths which can theoretically change under an imposed shear or extensional flow making the resulting flow behavior even more complex then polymeric fluids [Cates and Turner (1990)].

Viscoelastic wormlike micelle solutions are currently being used extensively as rheological modifiers in consumer products such as paints, detergents and pharmaceuticals where careful control of the fluid properties is required. In addition, micelle solutions have also become important in a wide range of applications including agrochemical spraying, inkjet printing and enhanced oil recovery. A fundamental understanding of the behavior of these complex fluids in different flow regimes is therefore extremely important to a host of industries. Techniques for the analysis and control of the flow of complex fluids require accurate determination of material properties as well as the ability to understand and predict changes that occur within the materials as they are subjected to the flow conditions encountered in industrial and commercial applications. Shear and extensional rheometers provide an excellent framework for investigating the behavior of these complex fluids because the flow kinematics tends to be simple. Additionally, these rheological measurements can shed light on phenomena such as elastic flow instabilities, which commonly occur in the many of the industrial and commercial applications mentioned above.

One of the observations that sparked the initial rheological interest in wormlike micelle solutions was that their linear viscoelastic response can often be quite accurately modeled by a Maxwell model having just a single relaxation time [Rehage and Hoffmann (1991)]. However, the nonlinear viscoelastic response of these entangled micelle solutions has been shown to be much more complex [Cates (1990); Khatory *et al.* (1993); Rothstein (2003)] and in need of further exploration.

The behavior of wormlike micelle solutions and other complex fluids in extensional flows is qualitatively different from their behavior in shear flows. The first experimental investigations of the apparent extensional rheology of wormlike micelle solutions used an opposed jet device [Fischer *et al.* (1997); Lu *et al.* (1998); Prud'homme and Warr (1994); Walker *et al.* (1996)]. Prud'homme and Warr (1994) showed for a series of equimolar

tetradecyltrimethylammonium bromide (TTABr)/Sodium Salicylate (NaSal) solutions that at low extension rates, below the coil-stretch transition, a plateau in the steady-state extensional viscosity was observed corresponding to the Newtonian response. At higher extension rates, chain stretching within the oriented segments was observed to lead to strain hardening in the extensional rheology. At a critical Deborah number, the extensional viscosity was observed to reach a maximum and decreases with further increases to the Deborah number. Prud'homme and Warr (1994) theorized that the observed reduction in the extensional viscosity at high extension rates was the result of a scission of the wormlike micelles in the strong extensional flow. This hypothesis was later supported by light scattering measurements [Chen and Warr (1997)] which demonstrated a decrease in the radius of gyration of the micelle with the reduction in the extensional viscosity and the filament stretching experiments of Rothstein (2003) which were able to quantify the energy required to scission wormlike micelles in strong extensional flows. Researchers have also used four-roll mills [Kato *et al.* (2002); Kato *et al.* (2004)] and the flow through porous media [Muller *et al.* (2004)] to measure an apparent extensional viscosity of wormlike micelle solutions.

In Anderson *et al.* (2004) and Yesilata *et al.* (2006), a capillary breakup extensional rheometer was used to measure the extensional viscosity of erucyl bis(hydroxyethyl)methylammonium chloride (EHAC) and iso-proponal in a brine of ammonium chloride in de-ionized water. Their results showed a strong extensional hardening for all of the surfactant and salt concentrations that they tested. Additionally, Yesilata *et al.* (2006) demonstrated that the extensional relaxation time, λ_E, extracted from intermediate decay of the fluid filament for the EHAC solutions was smaller by a factor of approximately 3 than the longest relaxation time obtained from oscillatory shear flow measurements, λ. This observation is very different from capillary breakup measurements of Boger fluids where these relaxation times were found to be approximately equal, $\lambda_E \approx \lambda$ [Anna and McKinley (2001)], in accordance with theoretical predictions of Entov and Hinch (1997).

In Rothstein (2003), a filament stretching rheometer was used to impose a uniaxial extensional flow on a series of solutions of cetyltrimethylammonium bromide (CTAB) and sodium salicylate (NaSal) while simultaneously making measurements of the evolution of the stress and flow induced birefringence (FIB) as a function of time and accumulated strain. These fluids were found to demonstrate considerable strain hardening in the elastic tensile stress and extensional viscosity [Chen and Rothstein (2004); Rothstein (2003)]. The filament stretching experiments were observed to come to an abrupt end with the rupture of the fluid filament near its axial midplane [Chen and Rothstein (2004); Rothstein (2003)]. Similar rupture events were also observed for associative polymer solutions in filament stretching experiments [Tripathi *et al.* (2006)] and wormlike micelle solutions in pendent drop experiments [Smolka and Belmonte (2003)]. At the surfactant concentrations used in these experiments, the wormlike micelles have been shown to be entangled forming heavily interconnected, sometimes branched, networks [Appell *et al.* (1992); Handzy and Belmonte (2004); In *et al.* (1999)]. This filament failure likely stems from the scission of wormlike micelles resulting in a dramatic breakdown of the micelle network structure *en masse* [Rothstein (2003)]. The failure of micelle solutions and associative polymer solutions in uniaxial extensional flows has also been found to lead to new and interesting instabilities in more complex flows such as in the extensional flow in the wake of a sphere falling through a wormlike micelle solution [Chen and Rothstein (2004); Jayaraman and Belmonte (2003)] or through an associative polymer solution [Mollinger *et al.* (1999)] and the extensional flow in the wake of a bubble rising through a wormlike micelle solution [Handzy and Belmonte (2004)]. These instabilities have great significance to industrial flows of wormlike micelle solutions such as in turbulent

drag reduction where strong extensional flow is often encountered. Much research is still needed if we are to truly understand the origins and implication of this new class of flow instabilities unique to self-assembling wormlike micelle solutions and associative polymer solutions.

Although the shear rheology of wormlike micelle solutions has been studied in great depth, only a relatively small number of extensional rheology measurements of wormlike micelle solutions currently exist in the literature. In the experiments described within this manuscript, filament stretching experiments are performed on two different surfactant solutions, namely CTAB/NaSal and CPyCl/NaSal, over a wide range of surfactant concentrations and extension rates. Extensional rheology results for a number of CTAB/NaSal solutions already exist in the literature [Rothstein (2003)]. In this manuscript, the previous filament stretching experiment of CTAB/NaSal solutions is extended to a number of previously untested surfactant concentrations. Additionally, in the experiments presented in this manuscript for both CTAB/NaSal and CPyCl/NaSal solutions, the extension rate is systematically varied and its role in the extensional rheology of the wormlike micelle solutions and the transition from elastocapillary failure to rupture of the fluid filaments is investigated. Last, the extensional rheology of the wormlike micelle solutions is measured using capillary breakup extensional rheology and the results are compared directly to those obtained through filament stretching. It is striking how poorly the extensional rheology measured with these two techniques agrees.

The outline of this paper is as follows. In Sec. II, we briefly describe the implementation of the filament stretching extensional rheometer and the capillary breakup extensional rheometer, the test fluids used and their shear rheology. In Sec. III A, we discuss the transient homogeneous uniaxial extensional rheology measured through filament stretching. In Sec. III B we discuss the extensional rheology of the test fluids measured through capillary breakup. Finally, in Sec. IV we conclude.

II. EXPERIMENTAL SETUP

A. Test fluids

A series of wormlike micelle solutions assembled from two different surfactant/salt combinations were chosen for this study. The first set of wormlike micelle solutions that were tested were made up of the cationic surfactant cetylpyridinium chloride (CPyCl) and sodium salicylate (NaSal) dissolved in a brine of 100 mM NaCl in distilled water. For reasons described in Miller and Rothstein (2006), the molar ratio of surfactant to the binding salt in this system was held fixed at [CPyCl]/[NaSal]=2. The addition of the salt helps screen the charges on the hydrophilic head groups of the surfactant making the resulting micelle more flexible [Kern *et al.* (1994)]. The electrostatic screening of the salt has been observed to lower the critical micellar concentration (CMC) for CPyCl in aqueous NaCl from $CMC_{CPy,H_2O}=0.90$ mM to $CMC_{CPy,NaCl}=0.12$ mM [Lee *et al.* (2005)]. CPyCl and NaSal were obtained in dry form from Fisher Scientific. Molar concentrations of CPyCl between 50 and 200 mM were dissolved in brine on a hot plate with a magnetic stirring bar. During mixing, a moderately elevated temperature was applied to reduce viscosity and aid in uniform mixing. After the solutions were fully dissolved, approximately 20–30 min, they were allowed to settle at room temperature for at least 24 h before any experiments were performed to allow air bubbles introduced during mixing to rise out.

The second set of test fluids were a series of wormlike micelle solutions made up of another cationic surfactant CTAB (Fisher Scientific) and NaSal (Fisher Scientific) in de-ionized water. As has been customary in the literature [Shikata and Kotaka (1991)],

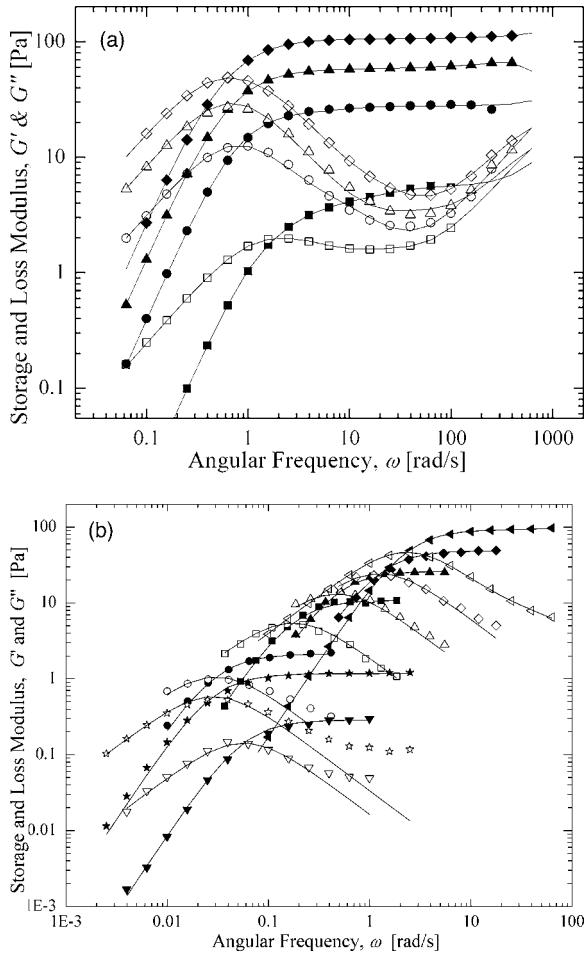

FIG. 2. Small amplitude oscillatory rheology of (a) CPyCl/NaSal solutions in 100 mM NaCl at $T=20$ °C and (b) CTAB/NaSal solution at $T=25$ °C. The data in (a) include: storage modulus, G' (filled symbols), and loss modulus, G'' (open symbols), for ■ 50/25 mM, ● 100/50 mM, ▲ 150/75 mM, and ♦ 200/100 mM with two-mode Maxwell model fits to each of the data sets (–). The data in (b) include: for ▼ 10/10 mM, ★ 17.5/17.5 mM, ● 25/25 mM, ■ 50/50 mM, ▲ 75/75 mM, ♦ 100/100 mM, and ◀ 150/150 mM with a single-mode Maxwell fits to each of the data sets (–).

the molar ratio of surfactant to the binding salt was held fixed at [CTAB]/[NaSal]=1 and for our experiments the molar concentration of the CTAB was varied from 10 and 150 mM. Each of these solutions is well above the critical micelle concentration, which for CTAB in pure water is CMC=0.9 mM and is again significantly lower in the presence of salt [Israelachvili (1985)]. The solutions were prepared as described above. For both solutions, at the concentrations used, the wormlike micelle solutions are concentrated and entangled with a significant number of entanglement points per chain [Israelachvili (1985)].

All extensional rheology experiments were performed at room temperature ($T=23\pm2$ °C). When analyzing and presenting the experimental data, the relaxation times and viscosities were adjusted to their values at a reference temperature of $T_0=25$ °C using time-temperature superposition with a shift factor, a_T, defined by the Arrhenius equation [Bird *et al.* (1987)]. Over the temperature range of our experiments,

TABLE I. Parameters characterizing the rheology of the CTAB/NaSal wormlike micelle solutions.

			CTAB/NaSal [mM]						
			10/10	17.5/17.5	25/25	50/50	75/75	100/100	150/150
Zero-shear viscosity	η_0	[Pa s]	5.0	41	68	62	55	39	38
Plateau modulus	G_0	[Pa]	0.28	1.2	2.5	10.9	26.2	48.8	94.8
Maxwell relaxation time	λ_M	[s]	18	35	27	5.7	2.1	0.8	0.4
Critical diameter	D^*	[mm]	173	41	19	4.4	1.8	0.98	0.51

the Arrhenius form of the time-temperature shift factor was found to be in good agreement with the rheological data for each of the wormlike micelle solutions tested.

B. Shear rheometry

The steady and dynamic shear rheology of the test fluids was characterized using a stress-controlled rheometer (TA instruments, AR2000) with a 6 cm/2° cone-and-plate geometry. The micelle solutions were loaded and allowed to equilibrate for several minutes. The samples were not presheared. In Fig. 2, the storage modulus, G', and loss modulus, G'', of the CPyCl/NaSal and the CTAB/NaSal wormlike micelle solutions were plotted as a function of angular frequency, ω, along with the prediction of a Maxwell model. The viscoelastic properties of the fluids listed in Tables I and II including zero shear rate viscosity, η_0, Maxwell relaxation time,λ_M, and the elastic plateau modulus, G_N^0, are found by fitting the data to a single-mode Maxwell model. The deviation of the rheological data from the predictions of the single-mode Maxwell model observed at large angular frequencies in Fig. 2(b) correspond to the Rouse-like behavior of the micelle between entanglement points [Fischer and Rehage (1997)]. This deviation, which has been shown to become more pronounced with increase in the concentration of surfactant/salt, is well predicted by adding a second mode, the Maxwell model as in Fig. 2(b) and can be used to determine both the breakup time, λ_{br}, and the reptation time, λ_{rep}, of the wormlike micelle chains. In the fast breaking limit $\lambda_{rep} \gg \lambda_{br}$, Cates showed that the breakup and reptation time could be related to the measured value of the Maxwell relaxation time through $\lambda_M = (\lambda_{rep}\lambda_{br})^{1/2}$ [Cates (1987)]. Additionally, the theoretical mesh size $\zeta_m = (kT/G_0)^{1/3}$ [Doi and Edwards (1986); Granek and Cates (1992)] can be determined in order to gain some information about the proximity of entanglement points and the density of the wormlike micelle mesh.

In Fig. 3, the steady shear viscosity, η, is plotted as a function of shear rate, $\dot{\gamma}$. At small shear rates and angular frequencies, the micelle solutions have a constant zero shear rate viscosity. As the shear rate is increased, the fluid begins to shear thin. At a critical

TABLE II. Parameters characterizing the rheology of the CPyCl/NaSal wormlike micelle solutions.

			CPyCl/NaSal [mM]			
			50/25	100/50	150/75	200/100
Zero-shear viscosity	η_0	[Pa s]	1.0	11	30	69
Plateau modulus	G_0	[Pa]	4.2	27	60	104
Maxwell relaxation time	λ_M	[s]	0.27	0.50	0.56	0.59
Critical diameter	D^*	[mm]	12	2.1	0.84	0.39

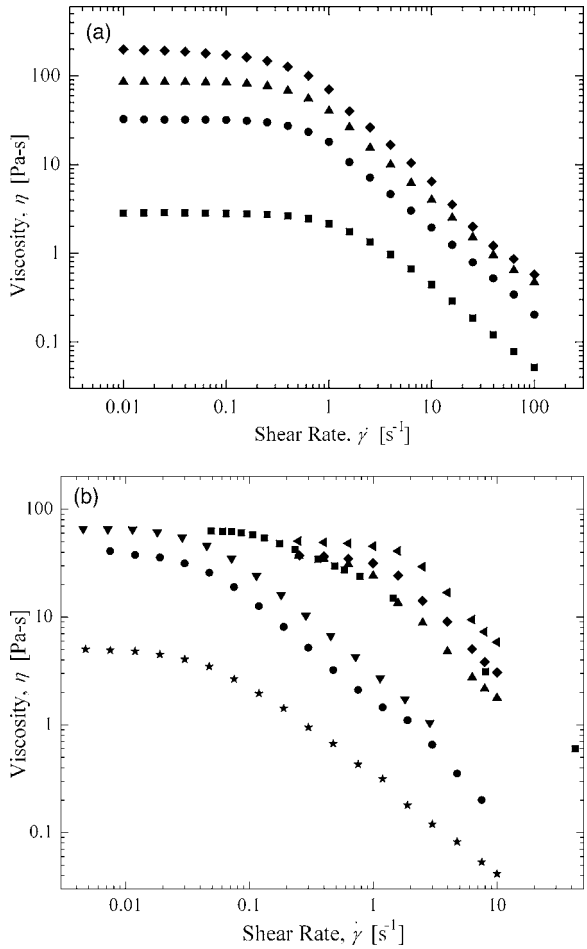

FIG. 3. Steady shear viscosity of (a) CPyCl/NaSal solutions in 100 mM NaCl at $T=20\,^{\circ}C$ and (b) CTAB/NaSal solution at $T=25\,^{\circ}C$. The data in (a) include: ■ 50/25 mM, ● 100/50 mM, ▲; 150/75 mM and ◆ 200/100 mM. The data in (b) include: for ▼; 10/10 mM, ★; 17.5/17.5 mM, ● 25/25 mM, ■; 50/50 mM, ▲; 75/75 mM, ◆; 100/100 mM, and ◀; 150/150 mM.

shear rate, the viscosity drops precipitously approaching a slope of $\eta \propto \dot{\gamma}^{-1}$. For the CPyCl/NaSal solutions, this plateau in the shear stress corresponds to the formation of two or more distinct shear bands. These shear bands have been recently measured and analyzed in our lab using particle image velocimetry and flow induced birefringence (FIB) measurements and a specially designed large Couette flow cell [Miller and Rothstein (2006)]. Although we have not yet attempted to observe shear banding in the CTAB/NaSal solutions, it could also account for the dramatic reduction in the shear viscosity observed in these systems.

C. Filament stretching extensional rheometry

A filament stretching extensional rheometer (FiSER) capable of imposing a homogeneous uniaxial extension on a fluid filament placed between its two end plates was used to make simultaneously measurements of the evolution in the force and the midpoint radius. A complete description of the design and operating space of the filament stretch-

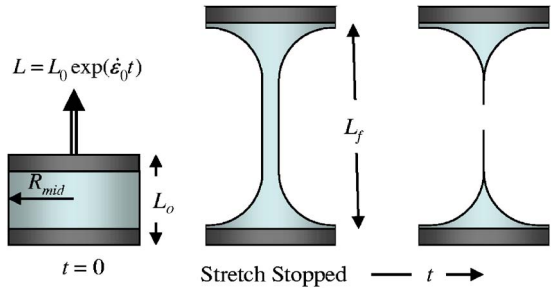

FIG. 4. Schematic diagram of capillary breakup extensional rheometry.

ing rheometer used in these experiments can be found in Rothstein and McKinley [Rothstein (2003); Rothstein and McKinley (2002a); Rothstein and McKinley (2002b)] and a more detailed history of the technique can be found in the following papers by the McKinley and Sridhar groups [Anna *et al.* (2001); McKinley and Sridhar (2002); Tirtaatmadja and Sridhar (1993)].

The goal of extensional rheometry is to cause a motion such that the resulting extension rate imposed on the fluid filament, $\dot{\varepsilon}$, is constant. The deformation imposed upon the fluid filament can be described in terms of a Hencky strain, $\varepsilon = -2\ln(R_{mid}/R_0)$, where R_0 is the initial midpoint radius of the fluid filament. The strength of the extensional flow is characterized by the Deborah number, $De = \lambda\dot{\varepsilon}$, which is the ratio of the characteristic relaxation time of the fluid, λ, to the characteristic time scale of the flow, $1/\dot{\varepsilon}_0$. The elastic tensile stress difference generated within the filament can be calculated from the algebraic sum of the total force measured by the load cell, F_z, if the weight of the fluid and the surface tension are taken into account while ignoring inertial effects [Szabo (1997)]

$$\langle \tau_{zz} - \tau_{rr} \rangle = \frac{F_z}{\pi R_{mid}^2} + \frac{1}{2}\frac{\rho g(\pi L_0 R_0^2)}{\pi R_{mid}^2} - \frac{\sigma}{R_{mid}}, \tag{1}$$

where L_0 is the initial end plate separation, σ is the equilibrium surface tension of the fluid and ρ is the density of the fluid. The extensional viscosity may be extracted from the principle elastic tensile stress and is often nondimensionalized as a Trouton ratio

$$Tr = \langle \tau_{zz} - \tau_{rr} \rangle / \eta_0 \dot{\varepsilon} = \eta_E^+ / \eta_0, \tag{2}$$

where η_E^+ is the transient extensional viscosity and η_0 is the zero shear rate viscosity of the fluid, respectively.

D. Capillary breakup extensional rheometry

In order to determine the extensional rheology of the less concentrated and less viscous fluids, capillary breakup extensional rheometry measurements [Anna and McKinley (2001); Bazilevsky *et al.* (1990); Entov and Hinch (1997); McKinley and Tripathi (2000); Rodd *et al.* (2005); Stelter *et al.* (2000)] were performed using the filament stretching rheometer described above [Rothstein (2003); Rothstein and McKinley (2002b)]. In a capillary breakup extensional rheometer (CaBER), an initial nearly cylindrical fluid sample is placed between the two end plates of the filament stretching rheometer and stretched with an exponential profile, $L = L_0 \exp(\dot{\varepsilon}_0 t)$, to final length of L_f. The stretch is then stopped and the capillary thinning of the liquid bridge formed between the two end plates produces a uniaxial extensional flow that can be used to measure an apparent

extensional viscosity. A schematic diagram of the stretch is shown in Fig. 4. The final stretch length is chosen such that $L_F = 3.6R_0$ and the stretch rate is chosen such that it is greater than the characteristic relaxation time of the fluid, $\dot{\varepsilon} \gg 1/\lambda$, and also greater than the time scale for capillary drainage of the liquid bridge, $\dot{\varepsilon} \gg \sigma/\eta_0 R_0$ [Anna and McKinley (2001)]. It has been shown that CaBER is capable of measuring the extensional viscosity of fluids with shear viscosities as low as 70 mPa s and relaxation times as low as 10 ms [Rodd *et al.* (2005)]. In addition, CaBER can reach extremely large Hencky strains limited only by the resolution of diameter measurement transducer. In our experiments, a laser micrometer (Omron Z4LA) with a resolution of 5 μm was used to obtain final Hencky strains of up to $\varepsilon = 2\ln(3\text{ mm}/5\ \mu\text{m}) = 12.7$, although in practice reliable measurements below 20 μm were difficult to achieve.

The breakup of the fluid filament is driven by capillary stresses and resisted by the extensional stresses developed within the flow. The extensional viscosity of the wormlike micelle solution can be determined by measuring the change in the filament diameter as a function of time. Papageorgiou (1995) showed that for a Newtonian fluid the radius of the fluid filament will decay linearly with time, $R_{mid}(t) \propto (t_b - t)$. Conversely, Entov and Hinch (1997) showed that for an Oldroyd-B fluid, the radius will decay exponentially with time, $R_{mid}(t) \propto \exp(-t/3\lambda_E)$. The extension rate of the fluid filament is given by

$$\dot{\varepsilon} = -\frac{2}{R_{mid}(t)}\frac{dR_{mid}(t)}{dt} = \frac{2}{3\lambda_E} \tag{3}$$

and hence for an Oldroyd-B fluid, the flow has a constant Deborah number of $De = 2/3$. This value is larger than the critical Deborah number of $De = 1/2$ needed to achieve coil-stretch transition and thus strain hardening of the extensional viscosity of the wormlike micelle solutions can be achieved. Additionally, the slope of the diameter as a function of time can be used to calculate a relaxation time in this elongational flow, λ_E. For Boger fluids, theory predictions and experiments show that $\lambda_E \approx \lambda$. An apparent extensional viscosity can be calculated by applying a force balance between capillary stresses and the elastic tensile stresses within the fluid filament [Anna and McKinley (2001)]

$$\eta_E = \frac{\sigma/R_{mid}(t)}{\dot{\varepsilon}(t)} = \frac{-\sigma}{dD_{mid}/dt}. \tag{4}$$

To calculate the extensional viscosity, the diameter measurements are fit with the functional form proposed by Anna and McKinley (2001),

$$D_{mid}(t) = Ae^{-Bt} - Ct + E, \tag{5}$$

and differentiated with respect to time. The choices of fitting parameters have their physical relevance. The decay of the fluid filament diameter at intermediate times can be related to the extensional relaxation time and the fitting parameter B such that $B = 1/3\lambda_E$. Additionally, C can be related to equilibrium value of the extensional viscosity such that $C = \sigma/\eta_{E,\infty}$.

The equilibrium surface tension for each of the wormlike micelle solutions tested was assumed to be consistent with the value of $\sigma = 0.032$ and 0.036 N/m reported in the literature for the CPyCl/NaSal and CTAB/NaSal solutions above the CMC, respectively [Akers and Belmonte (2006); Cooper-White *et al.* (2002)]. However, in any free surface flow containing surfactants, one must also consider the role that dynamic surface tension could play. As the fluid filament is stretched and a new surface is generated, surfactant molecules diffuse from the bulk and populate the new surface. The result is a surface

tension that is a function of the age of a given surface. Because the time scales of the CaBER experiments described here are slow compared to the time scale of the dynamic surface tension (seconds vs. milliseconds) [Cooper-White *et al.* (2002)] the equilibrium value of the surface tension was used in all of our calculations of the extensional viscosity. Additionally, in the FiSER experiments, at the point that the fluid filament is stretching fast enough to necessitate the use of the dynamic surface tension in the force balance in Eq. (1), the elastic tensile stress typically dominates over the surface tension term and the factor of 2 change in the surface tension would make little to no difference in the final value of the extensional viscosity.

III. RESULTS AND DISCUSSION

A. Filament stretching extensional rheometry

A series of constant extension rate experiments were performed on broad range of wormlike micelle solutions using the filament stretching rheometer described in Sec. II C. The spectrum of strain rates and final Hencky strains were designed to maximize the knowledge gained of the behavior of these wormlike micelle solutions in extensional flows.

A quantitative analysis of the extensional rheology for a series of wormlike micellar solutions of both CPyCl/NaSal and CTAB/NaSal was performed using a filament stretching extensional rheometer and are presented in Fig. 5. In Figs. 5(a)–5(c), the measured elastic tensile stress as a function of time for a broad series of extension rates is presented for CPyCl/NaSal concentrations of 100/50, 150/75, and 200/100 mM, respectively. The elastic tensile stress in the fluid filaments was observed to increase monotonically and demonstrate some degree of strain hardening. At large extension rates, $\dot{\varepsilon} \gg 1/\lambda$ the fluid filaments were all found to rupture. However, as the extension rate was reduced, the filaments began to fail through an elastocapillary thinning and pinch off. For the 150/75 and 200/100 mM solutions, the transition from rupture to capillary pinch off was found to be at Deborah numbers of approximately $De \approx 0.99$ and 0.74, respectively. For the case of the 100/50 mM solution, the fluid was always found to rupture for all the extension rates tested. For all of the experiments that ended with a filament rupture, the final maximum elastic stress that was achieved in the fluid filaments of each solution was found to be constant independent of extension rate. For the 100/50, 150/75, and 200/100 mM CPyCl/NaSal solutions the tensile stress at rupture was found to be $\Delta\tau_E \cong 7100$, 6900, and 6700 Pa, respectively. The similarity in these tensile stresses is coincidental. If the differences in the elasticity of each solution are accounted for by nondimensionalizing the elastic tensile stress at rupture with the plateau modulus, we find that $\Delta\tau_E/G$ decays monotonically from $\Delta\tau_E/G = 260$, 116, to 64 as the CPyCl concentration is increased from 100, to 150 and finally to 200 mM. This observation of a constant rupture stress independent of extension rate is consistent with observations made previously for the extensional viscosity and filament rupture of CTAB/NaSal solutions [Rothstein (2003)], although the dependence of the dimensionless tensile stress at rupture on surfactant concentration appears to be slightly stronger for the case of the CPyCl/NaSal solutions.

The dynamics of the filament rupture were captured and analyzed using a high-speed digital video camera (Phantom v.4.2) at a frame rate of 2000 fps. A time-lapse series of images for a rupture event of the 150/75 mM CPyCl/NaSal at a Deborah number of $De = 2.6$ is shown in Fig. 6 and is very similar to the rupture events observed for CTAB/NaSal systems [Chen and Rothstein (2002)]. Unlike capillary driven filament breakup instabilities, which have been observed to occur in weakly strain hardening fluids after

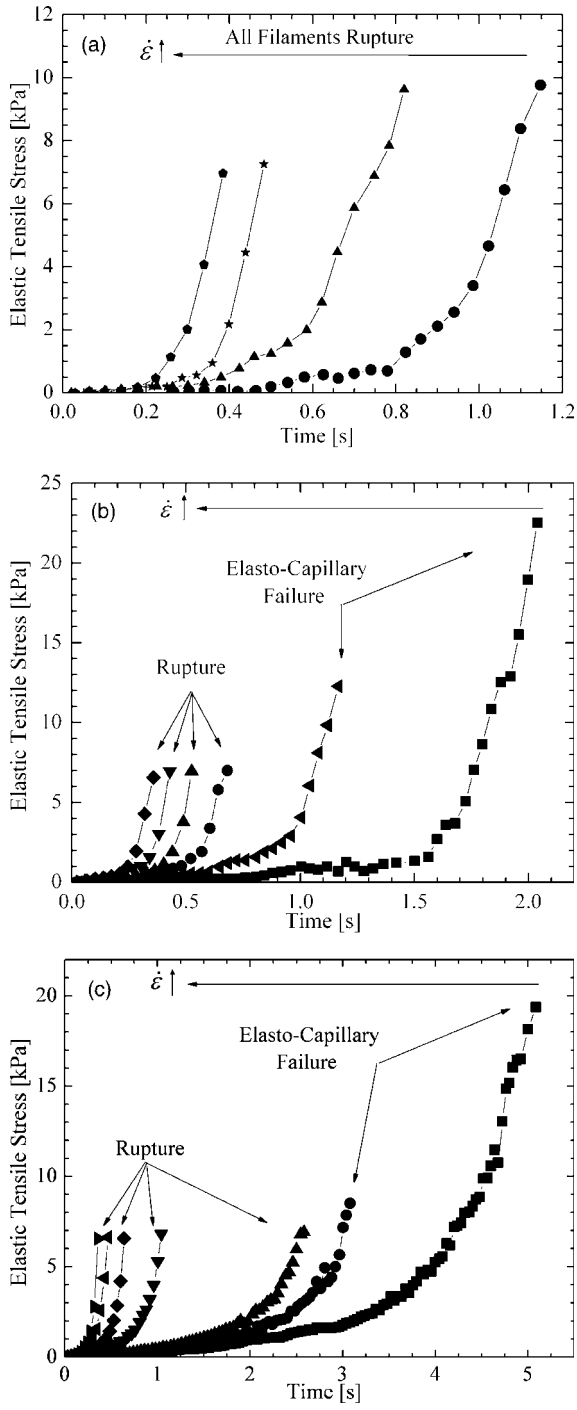

FIG. 5. Elastic tensile stress growth as a function of time for viscoelastic wormlike micelle solutions in uniaxial extensional flows at T_{ref}=25 °C. The figure includes data for: (a) 100/50 mM CPyCl/NaSal with increasing extension rates ranging from 2.6 $s^{-1} \leqslant \dot{\varepsilon} \leqslant 6.3\ s^{-1}$ ($1.3 \leqslant De \leqslant 3.2$); (b) 150/75 mM CPyCl/NaSal solution with extension rates ranging from 1.2 $s^{-1} \leqslant \dot{\varepsilon} \leqslant 4.2\ s^{-1}$ ($0.67 \leqslant De \leqslant 2.3$); and (c) 200/100 mM CPyCl/NaSal solution with extension rates ranging from 1.0 $s^{-1} \leqslant \dot{\varepsilon} \leqslant 6.0\ s^{-1}$ ($0.60 \leqslant De \leqslant 3.6$).

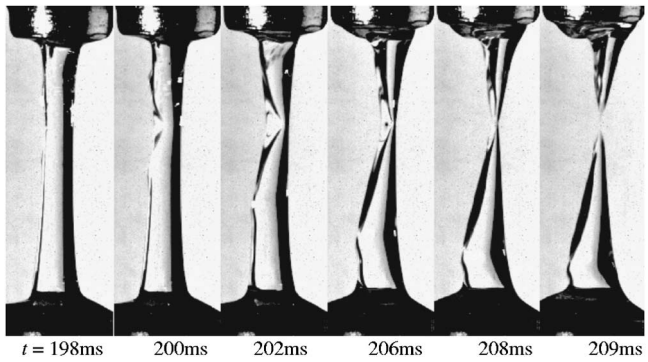

FIG. 6. Representative images of progressive filament rupture for the 150/75 mM CPyCl/NaSal solution at a $De=2.6$. The total duration of the failure event was determined to be 11 ms.

considerable necking of the fluid filament [Yao *et al.* (1998)], the failure of these wormlike micelle filaments occurs before any significant necking has occurred. The failure appears to be initiated by the growth of a surface or internal defect in the filament which rapidly propagates across the filament cleaving it in two. The propagation of defect and final failure of the fluid filament is quite rapid, taking only fractions of a second.

A review of the dynamics of the necking of viscoelastic fluid filaments was recently presented by Renardy (2004). In his review, Renardy showed that the purely elastic instabilities that we have observed in our experiments are independent of surface tension and can occur for fluids in which the extensional viscosity goes through a maximum with increasing strain. The observed filament failure mechanism appears similar to failures observed in tensile loading of elastic solids and extremely elastic polymer melts [Courtney (2000); Joshi and Denn (2003); Vinogradov *et al.* (1975)]. For the case of elastic solids, samples experiencing a uniform tensile deformation become unstable and fail when the force or the engineering stress goes through a maximum [Courtney (2000)]. At that point, the solid has exhausted its work-hardening capacity and begun to work soften, destabilizing any perturbation along the sample and producing a neck that grows rapidly with time. A similar breakup phenomenon was observed by Tripathi *et al.* (2006) during filament stretching experiments of a model associative polymer system containing hydrophobically modified ethoxylate-urathane. At high strain rates and Deborah numbers, Tripathi *et al.* (2006) observed the associative polymers exhibited a sudden rupture phenomenon while at low strain rates the filament was observed to fail through a visco-capillary thinning.

At lower Deborah numbers, where the fluid filament pinches off through elastocapillary thinning, the elastic tensile stress for both the 200/100 mM and 150/75 mM CPyCl/NaSal solutions were found to grow to values much larger than the critical stress for rupture. It has been hypothesized that the tensile stress of rupture corresponds to the maximum stress that the micelles can withstand before they begin to fail *en masse* [Rothstein (2003)]. One would therefore expect that as the extension rate is reduced and the filament transitions from rupture to capillary breakup, the final tensile stress would begin to decrease and not increase. Additionally, these observations for CPyCl/NaSal were not observed by Rothstein (2003) for CTAB/NaSal solutions. It is possible that this discrepancy may be because they simply did not probe the response of the CTAB/NaSal wormlike micelle solutions to low enough extension rates to observe a similar upturn in the stress. In order to test whether the response of the CPyCl/NaSal solution in exten-

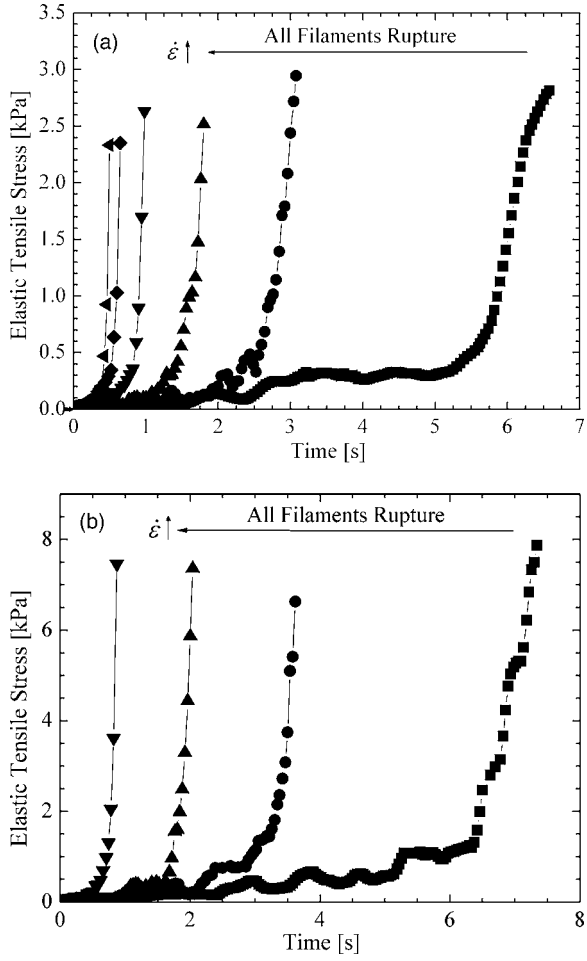

FIG. 7. Elastic tensile stress growth as a function of time for viscoelastic wormlike micelle solutions in uniaxial extensional flows at T_{ref}=25 °C. The figure includes data for (a) 50/50 mM CTAB/NaSal with increasing extension rates ranging from 0.13 $s^{-1} \leqslant \dot{\varepsilon} \leqslant 2.5\ s^{-1}$ ($0.75 \leqslant De \leqslant 14.3$); (b) 100/100 mM CTAB/NaSal solution with extension rates ranging from 0.7 $s^{-1} \leqslant \dot{\varepsilon} \leqslant 3.0\ s^{-1}$ ($0.6 \leqslant De \leqslant 2.4$).

sional flow is universal for all the wormlike micelle solutions or just a unique artifact of this particular system, a series of filament stretching experiments were performed for 50/50 and 100/100 mM CTAB/NaSal solutions to extend the range of extension rates imposed by Rothstein (2003).

In Figs. 7(a) and 7(b), the measured elastic tensile stress as a function of time for a broad series of extension rates is presented for CTAB/NaSal concentrations of 50/50 and 100/100 mM, respectively. The elastic tensile stress in the fluid filaments were all observed to increase monotonically and strain harden. For the 50/50 and 100/100 mM solutions, the filaments were found to rupture at each of the extension rates tested; even at extension rates corresponding to low Deborah numbers of De=0.75 and 0.6, respectively. The value of the tensile stress at rupture agrees well with the results of Rothstein (2003). The lack of an upturn in the tensile stress for the CTAB/NaSal solutions at low extension rates suggests that there may be a physical difference between the wormlike micelle solutions tested here. However, at the low Deborah numbers at which the upturn

is being measured, it is important to determine first that a constant extension rate profile was achieved and second that the experiments are affected by gravitational sagging. A careful inspection of the diameter profile as a function of time confirms that we are in fact achieving a constant extension rate profile. A more detailed analysis is required to understand the role of gravitational sagging on our experiments.

The useful operating space of the filament stretching rheometer is limited at large extension rates by the specifications of the rheometer and end plate instabilities [Spiegelberg and McKinley (1996)] and by gravitational sagging at low extension rates. The asymmetry in the initial fluid column is governed by the Bond number, $Bo=\rho g R_0^2/\sigma$, which is the ratio of gravitational to surface stresses. During stretch, the importance of gravitational sagging is governed by the ratio of the Bond number and the capillary number, $Bo/Ca=\rho g R_0/\eta_0\dot{\varepsilon}$, which expresses the ratio of gravitational and viscous forces during the stretch [Anna *et al.* (2001)]. When $Bo/Ca>1$, a significant amount of fluid can drain from the fluid filament to the bottom end plate during stretching. Thus, a minimum extension rate and Deborah number can be defined below which sagging becomes important

$$De_{sag}=\lambda\dot{\varepsilon}_{sag}=\lambda\rho g R_0/\eta_0. \tag{6}$$

For the CPyCl/NaSal solutions tested the critical Deborah number for the onset of gravitational sagging was $De_{sag}=1.1$, 0.46, and 0.21 for the 100/50, 150/75, and 200/100 mM solutions, respectively. It is clear, therefore, that none of the filament stretching experiments presented in Fig. 5 should be affected by gravitational sagging and it can be ruled out as the cause of the unexpected behavior observed at low extension rates.

For each of the experiments in Fig. 5, the Trouton Ratio was calculated from Eq. (4) and plotted as a function of accumulated Hencky strain in Fig. 8 for each of the CPyCl/NaSal solutions. With decrease in the imposed extension rate, we observe a delay in the strain hardening of the Trouton Ratio to larger Hencky strains. This is consistent with the response of both polymers and wormlike micelle solutions [McKinley and Sridhar (2002); Rothstein (2003)]. Owing to the constant elastic tensile stress achieved at rupture for the high Deborah number experiments, the Trouton ratio is found to decrease linearly with increasing imposed extension rate, $Tr\propto\dot{\varepsilon}^{-1}$. The Trouton Ratios at lower Deborah numbers increases sharply with decreasing extension rate as the filament transitions from rupturing to capillary failure.

This can be seen more clearly by plotting the maximum value of the extensional viscosity achieved either at the point of rupture or elastocapillary failure as a function of extension rate in Figs. 9 and 10 for the CPyCl/NaSal and CTAB/NaSal solutions, respectively. These plots also facilitate a comparison of our results to those obtained using an opposed jet device or a four-roll mill [Fischer *et al.* (1997); Kato *et al.* (2002); Kato *et al.* (2004); Lu *et al.* (1998); Prud'homme and Warr (1994); Walker *et al.* (1996)]. In Fig. 9(a), the 100/50 CPyCl/NaSal solutions did not demonstrate a transition from filament rupture to capillary pinch off, whereas this transition could be achieved for the 150/75 and 200/100 mM CPyCl/NaSal solutions respectively. As expected, the maximum extensional viscosity decays linearly with increasing strain rate at large extension rates. At lower extension rates, elastocapillary thinning is recovered and the filament is observed to achieve larger Hencky strains and extensional viscosities with decreasing extension rate. Extensional viscosity plots as a function of strain rate are also provided in Fig. 10 for both the 50/50 and 100/100 mM CTAB/NaSal solutions. For these fluids, the fluid filaments were observed to rupture at a critical stress for all the extension rates tested. Hence the slope of the maximum extensional viscosity as a function of the strain rate is

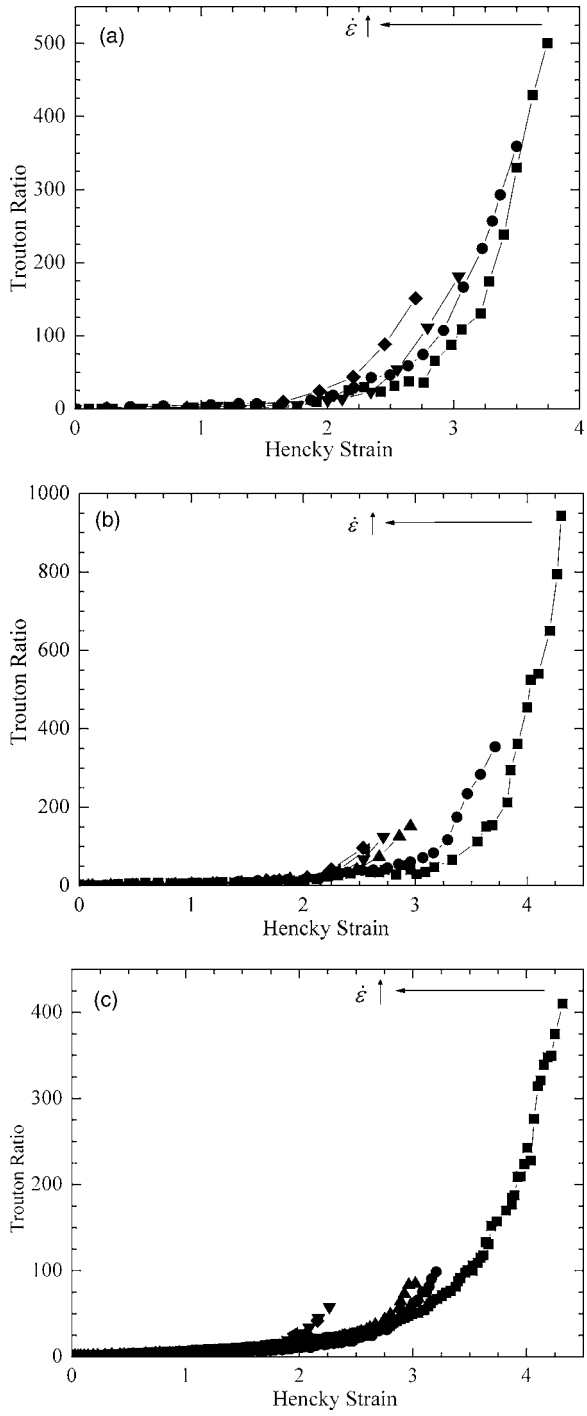

FIG. 8. The Trouton ratio as a function of the accumulated Hencky strain at T_{ref}=25 °C. The figure includes data for: (a) 100/50 mM CPyCl/NaSal with increasing extension rates ranging from 2.6 $s^{-1} \leqslant \dot{\varepsilon} \leqslant 6.3\ s^{-1}$ ($1.3 \leqslant De \leqslant 3.2$); (b) 150/75 mM CPyCl/NaSal solution with extension rates ranging from 1.2 $s^{-1} \leqslant \dot{\varepsilon} \leqslant 4.2\ s^{-1}$ ($0.67 \leqslant De \leqslant 2.3$); and (c) 200/100 mM CPyCl/NaSal solution with extension rates ranging from 1.0 $s^{-1} \leqslant \dot{\varepsilon} \leqslant 6.0\ s^{-1}$ ($0.60 \leqslant De \leqslant 3.6$).

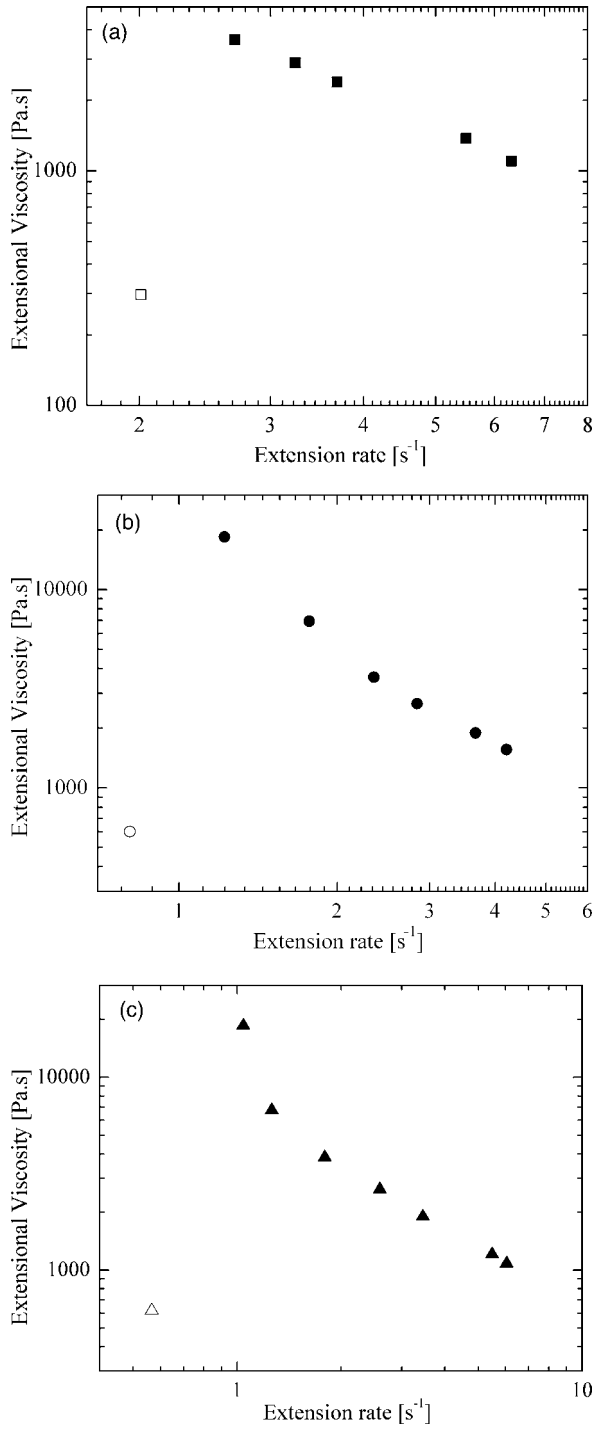

FIG. 9. The maximum extensional viscosity achieved either at filament rupture or elastocapillary pinch off as a function of the applied extension rate at T_{ref}=25 °C. Included in (a) are: ■ 100/50 mM CPyCl/NaSal; (b) ● 150/75 mM CPyCl/NaSal; and (c) ▲ 200/100 mM CPyCl/NaSal. The hollow symbols indicate plots for capillary breakup rheometry.

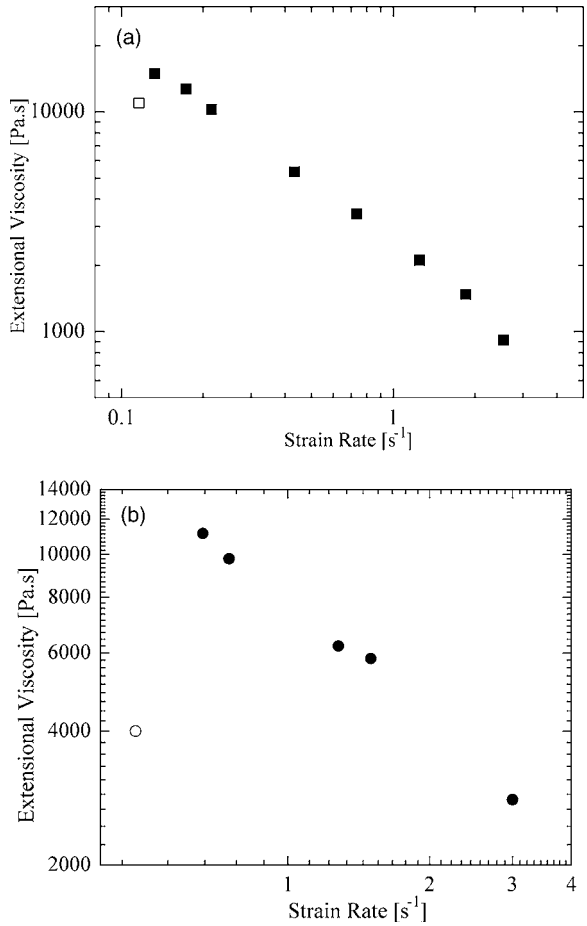

FIG. 10. The maximum extensional viscosity achieved either at filament rupture or elastocapillary pinch off as a function of the applied extension rate at T_{ref}=25 °C. Included in (a) are: ■ 50/50 mM CTAB/NaSal; and (b) ● 100/100 mM CTAB/NaSal. The hollow symbols indicate plots for capillary breakup rheometry.

found to be fixed at $Tr \propto \dot{\varepsilon}^{-1}$. On the basis of this observation, it may be inferred that there exist two distinct dynamic regimes of wormlike micelle solutions in extensional flows; elastocapillary thinning and filament rupture. Also included in Figs. 9 and 10 as hollow symbols are the apparent equilibrium extensional viscosities, for each of the fluids measured through capillary breakup extensional rheometry. We will discuss these experiments and the obvious discrepancies between the extensional viscosities measured between the filament stretching and capillary breakup in the following section.

B. Capillary breakup extensional rheometry

In capillary breakup extensional rheometry, the filament stretching rheometer was used to impose a step extensional strain on an initially cylindrical sample. The fluid filament was then allowed to thin under capillary motion as the diameter was monitored as a function of time. As described in Sec. II C, measurement of the diameter with time can be used to determine both an extensional relaxation time and an apparent transient extensional viscosity for fluids too thin to be measured using filament stretching. The dynamics of capillary thinning were captured and analyzed using a digital video camera. A series of

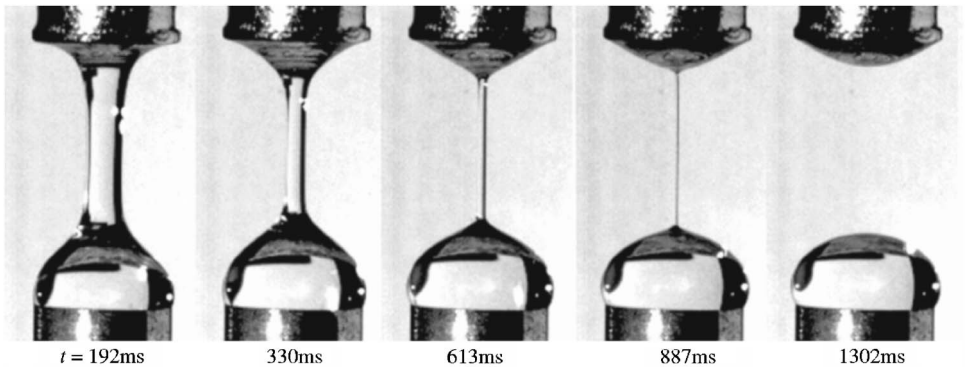

FIG. 11. Representative images of progressive filament failure, due to the influence of capillary action for the 50/25 mM CPyCl/NaSal solution.

time-lapse images for a capillary failure event of the 50/25 mM CPyCl/NaSal are shown in Fig. 11. The fluid filament initially forms a cylindrical fluid column between the two end plates and drains over time into semicircular blobs of fluid on each end plate and eventually pinching off after $t=1.3$ s. The effect of gravity can be observed in the disproportionate amount of the fluid on the bottom end plate.

Plots of diameter as a function of time are presented in Fig. 12 for the CPyCl/NaSal and CTAB/NaSal, respectively, along with a solid line corresponding to a best fit to Eq. (5). Using Eq. (5), the diameter data in Fig. 13(a) can be differentiated with respect to time and combined with the surface tension to produce an apparent transient extensional viscosity. We call this viscosity apparent because, unlike filament stretching experiments, the extension rate is not held fixed in these experiments, but rather changes as the effects of finite extensibility become more pronounced at larger strains. The decay of the diameter with time of the more concentrated solutions cannot be easily fit by Eq. (5). As the viscosity of the solution increases, the time during the early stretch that the fluid column remains Newtonian can be quite significant. At early times, the fluid response is Newtonian, $Tr=3$, and the diameter will decay linearly with time, $D(t)\sim D_0-\sigma t/3\eta_0$. The resulting extension rate increases with time, $\dot{\varepsilon}(t)=4\sigma/3D(t)\eta_0$, as the diameter decreases. Strain hardening of the extensional viscosity cannot begin until the Deborah number increases beyond $De=0.5$ and the micelles undergo a coil-stretch transition. Thus, a critical diameter can be inferred for the onset of capillary driven non-Newtonian extensional flow behavior and the onset of strain hardening

$$D^*=4\lambda\sigma/3\eta_0. \tag{7}$$

Thus for all the capillary breakup experiments shown in Fig. 13, the fit to Eq. (5) was only performed for diameters less than the critical diameter, D^*. Values of D^* for all of the fluids can be found in Tables I and II. Although the value of the critical diameter is typically large for the low concentration solutions, $D^*>D_0$, for the higher concentration solutions such as the 200/100 mM CPyCl/NaSal solution the critical diameter can get as small as $D^*=0.39$ mm. This analysis shows that there is an upper limit on the fluid elasticity, $G_0=\eta_0/\lambda$, for which CaBER is a viable for measuring extensional viscosities. The slope of the exponential decay of the curve for $D<D^*$ is a measure of the extensional relaxation time, λ_E, of the fluid as obtained from the coefficient of the exponent in Eq. (5).

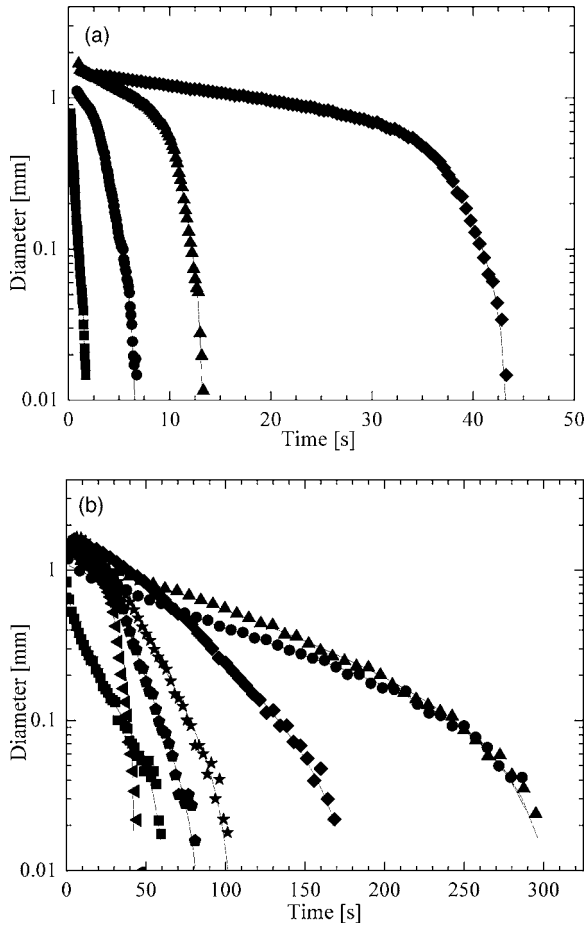

FIG. 12. Measurements of diameter as a function of time for a series of CABER experiments. Included in (a) are solutions of: ■ 50/25 mM, ● 100/50 mM, ▲ 150/75 mM; and ♦ 200/100 mM CPyCl/NaSal in 100 mM NaCl aqueous solution. Included in (b) are solutions of: ■ 10/10 mM, ● 17.5/17.5 mM, ▲ 25/25 mM, ♦ 50/50 mM, ξ 75/75 mM, — 100/100 mM, and ◄ 150/150 CTAB/NaSal in water.

A plot of the extensional relaxation time ratio measured from the CaBER experiments is plotted in Fig. 13 as a function of surfactant concentration. Yesilata *et al.* (2006) demonstrated that the extensional relaxation time extracted from intermediate decay of the fluid filament for the EHAC solutions was smaller by a factor of approximately 3 than the longest Maxwell relaxation time obtained from oscillatory shear rheology experiments, λ_M. This observation is different from capillary breakup measurements of Boger fluids where these relaxation times were found to be approximately equal, $\lambda_E=\lambda$ [Anna and McKinley (2001)] in accordance with the theoretical predictions of Entov and Hinch (1997). In the case of the CTAB/NaSal solutions, in Fig. 13(b) we observe the ratio of the extensional relaxation time to the Maxwell relaxation time, λ_E/λ_M, starts at values less than one and increases linearly with increasing surfactant concentration, eventually reaching a plateau at a value of approximately one, $\lambda_E/\lambda_M \cong 1$, for concentrations greater than CTAB $\geqslant$ 50 mM. For the case of CPyCl/NaSal solutions in Fig. 13(a), the ratio of

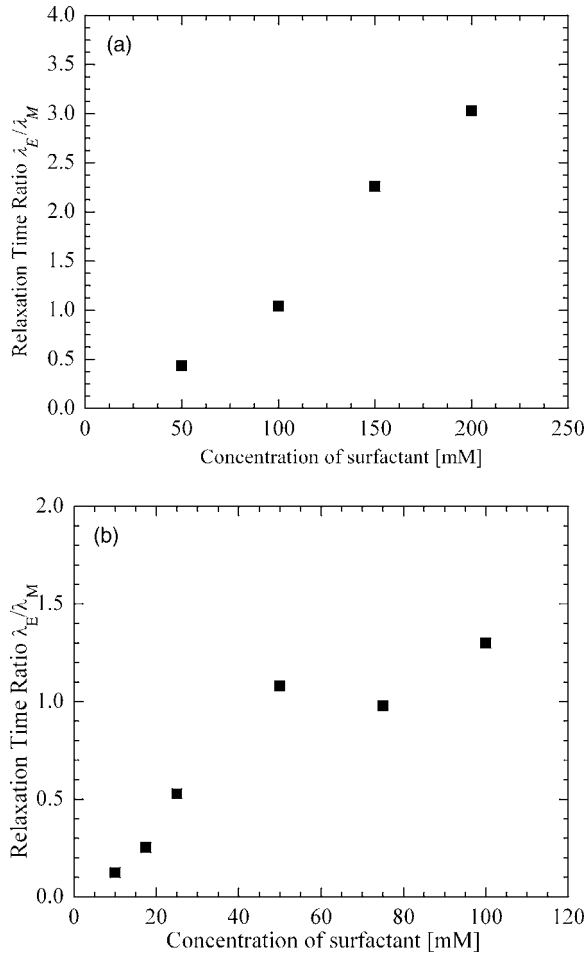

FIG. 13. Relaxation time ratio, λ_E/λ_M, as a function of surfactant/salt concentrations. Included in (a) are the CPyCl/NaSal solutions and in (b) are the CTAB/NaSal solutions.

the extensional to shear relaxation time also begins at a value much less than one, but then monotonically increases without reaching a similar plateau value at large surfactant concentrations.

The trends observed in the extensional relaxation times derived from the CaBER measurements, especially for the CTAB/NaSal solutions, may be a direct result of the initial Newtonian response of the fluid which may also play a large role in the explaining the discrepancies between CaBER and FiSER measurement of the extensional viscosity. The step strain imposed on the fluid filament to generate the liquid bridge in CaBER is essentially a pre-conditioning step that deforms the micelles parallel to the flow direction. The fluid is initially stretched at a very large extensional Deborah number, $De \gg 1$. The stretch is then stopped and the fluid filament is allowed to drain under a capillary action at a nominal Deborah number of $De=2/3$. The conventional wisdom in regards to CaBER measurements on polymer solutions is that the initial deformation induced by the step strain relaxes out quickly and does not affect the extensional rheology measurements as the CaBER experiment typically lasts order ten relaxation times [Anna and McKinley (2001)]. However, in self-assembled systems like wormlike micelle solutions, the initial

step strain can affect the size or morphology of the micelle or the interconnectivity of the micelle network probed by CaBER. This initial pre-conditioning step might account for the dramatic under prediction of the extensional relaxation time and equilibrium value of the extensional viscosity in the CaBER experiments when compared to the Maxwell relaxation time measured in shear and the maximum extensional viscosities measured in FiSER at similar extension rates, respectively. Recent studies by Bhardwaj *et al.* (2006), in which CTAB/NaSal and CPyCl/NaSal solutions were subjected to a precise amount of preshear prior to being stretched either with CaBER or FiSER, demonstrated that the extensional viscosity of these wormlike micelle solutions is extremely sensitive to even the smallest amounts of pre-conditioning, be that pre-shear or, in the case of CaBER and the studies presented here, pre-stretch. What is more, for the more concentrated solutions, the capillary drainage of the fluid filament at early times results in an extensional flow where $De \ll 1$. It is not until $D < D^*$ that the extensional flow becomes strong enough to begin to extend and stretch the micelles. For the more concentrated solutions, the time required to achieve D^* is often much greater than the relaxation time of the fluid. For these solutions, the early low Deborah number flow might allow the deformation and morphological changes imposed by the initial step strain to partially or even completely relax out. This would explain why the extensional relaxation time for CTAB/NaSal begins so much lower than the Maxwell relaxation time, but then recovers to the Maxwell relaxation time as the concentration of surfactant is increased and D^* is subsequently reduced. This argument does not, however, explain why the extensional relaxation time increases beyond the Maxwell relaxation time for the CPyCl/NaSal solutions with increasing surfactant concentration. For the higher concentration of CPyCl/NaSal solutions, it appears that the pre-stretch builds up structure in the wormlike micelle solutions rather than breaking it down.

A plot of the apparent Trouton ratio calculated from Eq. (4) for the CPyCl/NaSal and CTAB/NaSal wormlike micelle solutions is presented in Fig. 14. It may be observed that one of the primary advantages of using capillary breakup rheometry is that, apart from our ability to determine the extensional rheological properties of very low viscosity fluids, Hencky strains of the order of $\varepsilon = 2 \ln(R_0/R_{mid}(t)) \simeq 12$ can be achieved. This is in contrast to filament stretching rheology where the total imposed Hencky strains are limited by the travel of the end plates and filament rupture was typically observed to occur at values of Hencky strain less than $\varepsilon \leqslant 4$. The extensional viscosity of each of the fluids was found to strain harden and approached an equilibrium value at large Hencky strains. It should be noted that none of the extensional viscosities measured with filament stretching experiments achieved equilibrium, including the samples that did not rupture, but experienced an elastocapillary pinch off. This is most likely a result of the large Hencky strains that can be achieved with this technique. The value of the Trouton ratio was found to increase with decreasing surfactant concentration at the lower concentrations tested. This is consistent with previous literature which showed that for both entangled wormlike micelle solutions and entangled polymer solutions, that the degree of strain hardening decreases with increasing concentrations [Rothstein (2003); Rothstein and McKinley (2002a)]. Physically, this can be explained by considering that, as the concentration of surfactant is increased, the number of entanglement points along a wormlike chain increases and the molecular weight between entanglements decreases. This reduces the finite extensibility of the chain between entanglement points and therefore the equilibrium value of the Trouton ratio at a fixed Deborah number. The slight deviations from this trend for 25/25 mM CTAB/NaSal concentration is most likely a result of the large variation in the data from experiment to experiment and the error incurred while calcu-

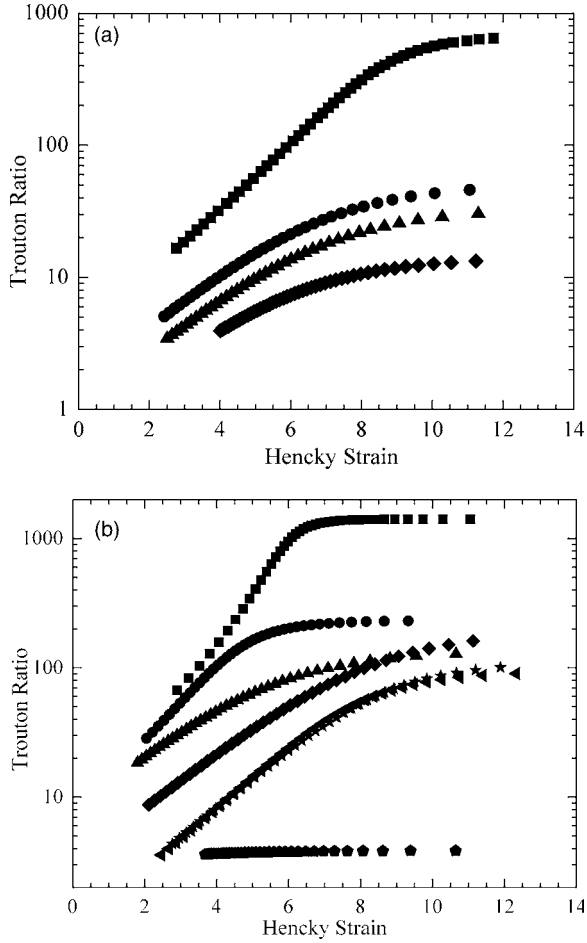

FIG. 14. CABER measurements of Trouton Ratio as a function of accumulated Hencky strain. Included in (a) are solutions of: ■ 50/25 mM, ● 100/50 mM, ▲ 150/75 mM; and ♦ 200/100 mM CPyCl/NaSal in 100 mM NaCl aqueous solution. Included in (b) are solutions of: ■ 10/10 mM, ● 17.5/17.5 mM, ▲ 25/25 mM, ♦ 50/50 mM, and ★ 75/75 mM, ◀ 100/100 mM, and 150/150 CTAB/NaSal in water.

lating the apparent extensional viscosity from the decay of the diameter with time. This is very different from the FiSER results that are very repeatable and have significantly less error in the extensional viscosity measurements.

The expected increase in the Trouton ratio with decreasing concentration can be seen more clearly if we think about the asymptotic analysis of the FENE-P model that the steady-state extensional viscosity can be written in the form [Doyle *et al.* (1998)]

$$\eta_{E,\infty} - 3\,\eta_s = 2nk_BT\lambda L^2(1 - 1/(2\lambda\dot{\varepsilon}) + \dots). \tag{8}$$

In CaBER experiments, the extension rate is nominally given by $\dot{\varepsilon}=2/3\lambda$ and furthermore the solvent contribution to the viscosity is essentially zero. Hence Eq. (8) reduces to $\eta_{E,\infty}=nk_BT\lambda L^2/2$. If we compare this value to that expected from filament stretching where the Deborah number is very large, we expect that $\eta_{E,\infty}(De=\infty)/\,\eta_{E,\infty}(De=2/3)=4$. Of course this is not quite right because Eq. (8) assumes a large value of the Deborah number. A full FENE-P uniaxial extensional flow simulation gives a ratio that is closer to a value of three assuming a zero stress initial condition for

the CaBER experiments. If, however, we plot the steady-state extensional viscosity measurements obtained using CaBER against the maximum values of extensional viscosity measured at filament rupture or elastocapillary failure with FiSER in Figs. 9 and 10, the results do not agree with the predictions of the FENE-P model. This is not completely unexpected considering that the FENE-P model was developed to describe the rheology of dilute polymer solutions not entangled wormlike micelle solutions. What is unexpected is how dramatically the FiSER and CaBER data differ at comparable extension rates. It is clear that a new differential constitutive model specifically derived for wormlike micelle solutions is needed if we are to accurately predict the behavior of these solutions in extensional flows.

A close inspection of Fig. 10 shows that the results of CaBER underpredict the extensional viscosity of the CTAB/NaSal solutions measured by FiSER by a factor of 2 or 3. Although not quantitative, the difference could be the result, at least in some part, of the dynamic surface tension of the surfactant solution. In calculating the apparent extensional viscosity from Eq. (4), the equilibrium value of the surface tension was used. If the surface tension of water were used, CaBER and FiSER data would compare more favorably. When these observations are taken in conjunction with the recovery of the extensional relaxation time at large surfactant concentrations, they suggest that the stresses and any morphological changes to the wormlike micelles resulting from the initial step stretch appear to relax out during the early stages of the capillary driven flow when $D < D^*$ and $De < \frac{1}{2}$.

As seen in Fig. 9, the discrepancy between the extensional viscosity of the CPyCl/NaSal solutions measured with CaBER and FiSER is dramatic and is clearly not the result of dynamics surface tension. Even for the 100/50 mM CPyCl/NaSal, which does not show the dramatic upturn in the extensional viscosity at low extension rates, the results from CaBER for the equilibrium value of the extensional viscosity are more than an order of magnitude less than the maximum value measured with FiSER. What is more remarkable is that none of the filament stretching experiments obtain a steady-state value of the extensional viscosity before they pinch off or rupture. This suggests that the difference in the steady-state extensional viscosity between these experiments is even larger than reported in Figs. 9 and 10. The disparity between the CaBER and FiSER results gets even worse for the 150/75 and 200/100 mM CPyCl/NaSal data for which the FiSER data shows a dramatic upturn in the extensional viscosity as the fluid filament transitions from rupture at large extension rates to elastocapillary failure as the extension rate is reduced below a critical value.

The dramatic difference between the extensional viscosities measured with CaBER and FiSER suggests that for wormlike micelle solutions the difference in the dynamics in these two uniaxial extensional flow experiments is extremely important. The flow imposed in FiSER is a transient homogeneous uniaxial extensional flow while CaBER, even after the step strain, is not homogeneous. Judging by the sensitivity of the extensional viscosity on extension rate, this difference may be enough to produce the observed differences in the data. The upturn in the extensional viscosity of the more concentrated solutions measured with FiSER as the extension rate is reduced suggests a change in the micelle dynamics, morphology, and/or aggregation number with extension rate. Micelles can only support a maximum stress before scission occurs [Rothstein (2003)]. Although micelles are continuously breaking and reforming, the likehood of micelle scission increases with increasing elastic tensile stress. When the wormlike micelles breaks, the newly formed cylindrical end caps are pulled apart by a combination of the extensional flow kinematics and the elastic recoil of the wormlike micelle. If the extension rate is

large enough, the end caps may pull apart too quickly to reform. Where these individual micelles break, the entangled wormlike micelle network is weakened locally and if enough micelles break *en masse* the fluid filament can rupture.

Since none of the CaBER experiments failed through rupture, a transition in FiSER from rupture to elastocapillary failure was expected as the extension rate imposed on the fluid filament in FiSER is reduced. As the extension rate is reduced, Eq. (2) demonstrates that a smaller tensile stress is needed to achieve the same extensional viscosity. One would therefore expect that the transition from rupture to elastocapillary failure would occur when the equilibrium value of the extensional viscosity can be reached without exceeding the tensile stress at rupture. At this point, we expected that the fluid filament would smoothly transition from rupture to an elastocapillary pinch off and that the measured extensional viscosity would display a maximum [Prud'homme and Warr (1994)] and then approach the CaBER results as the extension rate was further reduced as predicted by Eq. (8). Instead, the transition from rupture to elastocapillary failure for the 150/75 and 200/100 mM CPyCl/NaSal solutions was accompanied by a significant increase in the elastic tensile stress supported by the fluid filament far beyond the tensile stress that was found to result in rupture at larger extension rates. There are a number of possible explanations for the observed upturn in the extensional viscosity. As the extension rate is reduced and the flow kinematics are slowed down, individual micelles may have time to reattach or heal after a scission event even at stresses beyond the rupture stress observed at large extension rates. Alternatively, at these lower extension rates, the entangled wormlike micelle network may have enough time to rearrange itself in such a way as to increase the percentage of wormlike micelles actively carrying the axial stress accumulated within the fluid filament thereby increasing the critical stress required for rupture of the fluid filament. This hypothesis is further reinforced by the increase in the extensional relaxation time well above the Maxwell relation times for the CPyCl/NaSal solutions that demonstrate the upturn in the extensional viscosity. No matter which explanation is correct, what is clear is that the dynamics of FiSER and CaBER can produce very different responses from wormlike micelle solutions in extensional flows.

IV. CONCLUSIONS

In this work we report the result of both a filament stretching rheometer and capillary breakup rheometer used to measure the transient extensional rheology of a series of wormlike micelle solutions in uniaxial elongation flows. The experiments are performed using a series of wormlike micelle solutions of both cetylpyridinium chloride and sodium salicylate in an aqueous sodium chloride solution and cetyltrimethylammonium bromide and sodium salicylate in de-ionized water. All of the wormlike micelle solutions tested demonstrated single-mode or two-mode Maxwell behavior in small-amplitude oscillatory shear experiments and shear banding at large shear rates in steady-shear experiments.

In transient homogeneous uniaxial extension, all of the wormlike micelle solutions demonstrated significant strain hardening, the degree of which was found to increase with decreasing surfactant concentration. Above a critical extension rate, all of the wormlike micelle solution filaments tested were observed to fail through a dramatic rupture near the axial midplane. For each fluid, this failure was found to occur at a constant elastic tensile stress independent of imposed extension rate resulting in an extensional viscosity that was found to decay linearly with increasing extension rate. This filament failure likely stems from the local scission of individual wormlike micelles in the fluid filament *en masse*. For the less concentrated solutions, the fluid filaments were always found to rupture even as the Deborah number approached one half. For some of the more concen-

trated solutions, as the imposed extension rate was reduced, a critical extension rate was found below which the filament did not rupture, but instead elastocapillary thinning was recovered. For these cases, the elastic tensile stresses were measured within the fluid filament and therefore the extensional viscosity was found to grow far beyond the values observed at rupture. We hypothesized that this dramatic increase in the extensional viscosity at low extension rates is most likely the result of changes to the entangled wormlike micelle structure which enable a larger percentage of chains to carry extensional stress at lower extension rates. Strain hardening was also observed in capillary breakup rheometry experiments, however, a clear upper limit in the elastic modulus of the fluid was found for capillary breakup experiments. When the results of filament stretching and capillary breakup rheometry measurements at nominally the same extension rate were compared, the results do not agree; the extensional viscosity measurements from filament stretching are in some instances more than an order of magnitude larger than the capillary breakup measurements. This result demonstrates the sensitivity of these self-assembling wormlike micelle solutions to the dynamics of the extensional flow and brings into question the viability of using capillary breakup experiments to accurately measure the extensional viscosity of wormlike micelle solutions.

ACKNOWLEDGMENTS

We would like to thank the National Science Foundation for their generous support of this research under Grant Nos. CTS-0421043 and DMS-0406224.

References

Akers, B., and A. Belmonte, "Impact dynamics of a solid sphere falling into a viscoelastic micellar fluids," J. Non-Newtonian Fluid Mech. **135**, 97–108 (2006).

Anderson, V. J., P. M. J. Tardy, J. P. Crawshaw, and G. C. Maitland, "Extensional flow of wormlike micellar fluids," in *Int. Congr. Rheol.*, Seoul, Korea, 2004.

Anna, S. L., and G. H. McKinley, "Elasto-capillary thinning and breakup of model elastic liquids," J. Rheol. **45**, 115–138 (2001).

Anna, S. L., G. H. McKinley, D. A. Nguyen, T. Sridhar, S. J. Muller, J. Huang, and D. F. James, "An inter-laboratory comparison of measurements from filament stretching rheometers using common test fluids," J. Rheol. **45**, 83–114 (2001).

Appell, J., G. Porte, A. Khatory, F. Kern, and S. J. Candau, "Static and dynamic properties of a network of wormlike surfactant micelles (etylpyridinium chlorate in sodium chlorate brine)," J. Phys. II **2**, 1045–1052 (1992).

Bazilevsky, A. V., V. M. Entov, and A. N. Rozhkov, "Liquid filament microrheometer and some of its applications," in *Proc. Third European Rheology Conference*, Edinburgh, 1990.

Bhardwaj, A., D. Richter, M. Chellamuthu, and J. P. Rothstein, "The effect of preshear on the extensional rheology of wormlike micelle solutions," Rheol. Acta (2007) (in press).

Bird, R. B., R. C. Armstrong, and O. Hassager, *Dynamics of Polymeric Liquids: Volume 1 Fluid Mechanics* (John Wiley & Sons, New York, 1987).

Cates, M. E., "Reptation of living polymers: Dynamics of entangled polymers in the presence of reversible chain-scission reactions," Macromolecules **20**, 2289–2296 (1987).

Cates, M. E., "Nonlinear viscoelasticity of wormlike micelles (and other reversibly breakable polymers)," J. Phys. Chem. **94**, 371–375 (1990).

Cates, M. E., and M. S. Turner, "Flow-induced gelation of rodlike micelles," Europhys. Lett. **11**, 681–686 (1990).

Chen, C., and G. G. Warr, "Light scattering from wormlike micelles in an elongational flow," Langmuir **13**,

1374–1376 (1997).

Chen, S., and J. P. Rothstein, "Extensional flow of a wormlike micelle solution past a sedimenting sphere," in *Society of Rheology 74th Annual Meeting*, Minneapolis, MN, 2002.

Chen, S., and J. P. Rothstein, "Flow of a wormlike micelle solution past a falling sphere," J. Non-Newtonian Fluid Mech. **116**, 205–234 (2004).

Cooper-White, J. J., R. C. Crooks, and D. V. Boger, "A drop impact study of worm-like viscoelastic surfactant solutions," Colloids Surf., A **210**, 105–123 (2002).

Courtney, T. H., *Mechanical Behavior of Materials* (McGraw–Hill, Boston, 2000).

Doi, M., and S. F. Edwards, *The theory of polymer dynamics* (Oxford University Press, Oxford, 1986).

Doyle, P. S., E. S. G. Shaqfeh, G. H. McKinley, and S. H. Spiegelberg, "Relaxation of dilute polymer solutions following extensional flow," J. Non-Newtonian Fluid Mech. **76**, 79–110 (1998).

Entov, V. M., and E. J. Hinch, "Effect of a spectrum of relaxation times on the capillary thinning of a filament of elastic liquid," J. Non-Newtonian Fluid Mech. **72**, 31–53 (1997).

Fischer, P., G. G. Fuller, and Z. Lin, "Branched viscoelastic surfactant solutions and their responses to elongational flow," Rheol. Acta **36**, 632–638 (1997).

Fischer, P., and H. Rehage, "Rheological master curves of viscoelastic surfactant solutions by varying the solvent viscosity and temperature," Langmuir **13**, 7012–7020 (1997).

Granek, R., and M. E. Cates, "Stress relaxation in living polymers: Results from a Poisson renewal model," J. Chem. Phys. **96**, 4758–4767 (1992).

Handzy, N. Z., and A. Belmonte, "Oscillatory rise of bubbles in wormlike micellar fluids with different microstructures," Phys. Rev. Lett. **92**, 124501 (2004).

In, M., G. G. Warr, and R. Zana, "Dynamics of branched threadlike micelles," Phys. Rev. Lett. **83**, 2278–2281 (1999).

Israelachvili, J. N., *Intermolecular and Surface Forces: With Applications to Colloidal and Biological Systems* (Academic, London, 1985).

Jayaraman, A., and A. Belmonte, "Oscillations of a solid sphere falling through a wormlike micelle solution," Phys. Rev. E **67**, 065301 (2003).

Joshi, Y. M., and M. M. Denn, "Rupture of entangled polymeric liquids in elongational flows," J. Rheol. **47**, 291–298 (2003).

Kato, M., T. Takahashi, and M. Shirakashi, "Steady planar elongational viscosity of ctab/nasal aqueous solutions measured in a 4-roll mill flow cell," J. Soc. Rheol., Jpn. **30**, 283–287 (2002).

Kato, M., T. Takahashi, and M. Shirakashi, "Flow-induced structure change and flow instability of ctab/nasal aqueous solution in 4-roll mill flow cell," in *Int. Congr. on Rheol.*, Seoul, Korea, 2004.

Kern, F., F. Lequeux, R. Zana, and S. J. Candau, "Dynamics properties of salt-free viscoelastic micellar solutions," Langmuir **10**, 1714–1723 (1994).

Khatory, A., F. Lequeux, F. Kern, and S. J. Candau, "Linear and nonlinear viscoelasticity of semidilute solutions of wormlike micelles at high salt concentration," Langmuir **9**, 1456–1464 (1993).

Larson, R. G., *The Structure and Rheology of Complex Fluids* (Oxford University Press, New York, 1999).

Lee, J. Y., G. G. Fuller, N. E. Hudson, and X.-F. Yuan, "Investigation of shear-banding structure in wormlike micellar solution by point-wise flow-induced birefringence measurements," J. Rheol. **49**, 537–550 (2005).

Lequeux, F., and S. J. Candau, "Structural properties of wormlike micelles," In: *Theoretical Challenges in the Dynamics of Complex Fluids* (Kluwer, Dordrecht, 1997).

Lu, B., X. Li, L. E. Scriven, H. T. Davis, Y. Talmon, and J. L. Zakin, "Effect of chemical structure on viscoelasticity and extensional viscosity of drag-reducing cationic surfactant solutions," Langmuir **14**, 8–16 (1998).

McKinley, G. H., and T. Sridhar, "Filament stretching rheometry," Annu. Rev. Fluid Mech. **34**, 375–415 (2002).

McKinley, G. H., and A. Tripathi, "How to extract the Newtonian viscosity from capilary breakup measurements in a filament rheometer," J. Rheol. **44**, 653–670 (2000).

Miller, E., and J. P. Rothstein, "Transient evolution of shear banding in wormlike micelle solutions," J. Non-Newtonian Fluid Mech. (2007) (in press).

Mollinger, A. M., E. C. Cornelissen, and B. H. A. A. van den Brule, "An unexpected phenomenon observed in

particle settling: Oscillating falling spheres," J. Non-Newtonian Fluid Mech. **86**, 389–393 (1999).

Muller, A. J., M. F. Torres, and A. E. Saez, "Effect of the flow field on the rheological behavior of aqueous cetyltrimethylammonium *p*-toluenesulfonate solutions," Langmuir **20**, 3838–3841 (2004).

Olmsted, P. D., "Dynamics and flow induced phase separation in polymeric fluids," Curr. Opin. Colloid Interface Sci. **4**, 95–100 (1999).

Papageorgiou, D. T., "On the breakup of viscous liquid threads," Phys. Fluids **7**, 1529–1544 (1995).

Prud'homme, R. K., and G. G. Warr, "Elongational flow of solutions of rodlike micelles," Langmuir **10**, 3419–3426 (1994).

Rehage, H., and H. Hoffmann, "Viscoelastic surfactant solutions: Model systems for rheological research," Mol. Phys. **74**, 933–973 (1991).

Renardy, M., "Self-similar breakup of non-Newtonian fluid jets," In *Rheology Reviews*, edited by D. M. Binding and K. Walters (The British Society of Rheology, Aberystwyth, UK, 2004).

Rodd, L. E., T. P. Scott, J. J. Cooper-White, and G. H. McKinley, "Capillary break-up rhemetry of low-viscosity elastic fluids," Appl. Rheol. **15**, 12–27 (2005).

Rothstein, J. P., "Transient extensional rheology of wormlike micelle solutions," J. Rheol. **47**, 1227–1247 (2003).

Rothstein, J. P., and G. H. McKinley, "A comparison of the stress and birefringence growth of dilute, semi-dilute and concentrated polymer solutions in uniaxial extensional flows," J. Non-Newtonian Fluid Mech. **108**, 275–290 (2002a).

Rothstein, J. P., and G. H. McKinley, "Inhomogeneous transient uniaxial extensional rheometry," J. Rheol. **46**, 1419–1443 (2002b).

Shikata, T., and T. Kotaka, "Entanglement network of thread-like micelles of a cationic detergent," J. Non-Cryst. Solids **131–133**, 831–835 (1991).

Smolka, L. B., and A. Belmonte, "Drop pinch-off and filament dynamics of wormlike micellar fluids," J. Non-Newtonian Fluid Mech. **115**, 1–25 (2003).

Spiegelberg, S. H., and G. H. McKinley, "Stress relaxation and elastic decohesion of viscoelastic polymer solutions in extensional flow," J. Non-Newtonian Fluid Mech. **67**, 49–76 (1996).

Stelter, M., G. Brenn, A. L. Yarin, R. P. Singh, and F. Durst, "Validation and application of a novel elongational device for polymer solutions," J. Rheol. **44**, 595–616 (2000).

Szabo, P., "Transient filament stretching rheometry *i*: Force balance analysis," Rheol. Acta **36**, 277–284 (1997).

Tirtaatmadja, V., and T. Sridhar, "A filament stretching device for measurement of extensional viscosity," J. Rheol. **37**, 1133–1160 (1993).

Tripathi, A., G. H. McKinley, K. C. Tam, and R. D. Jenkins, "Rheology and dynamics of associative polymers in shear and extension: Theory and experiments," Macromolecules **39**, 1981–1999 (2006).

van Egmond, J. W., "Shear-thickening in suspensions, associating polymers, worm-like micelles and polymer solutions," Curr. Opin. Colloid Interface Sci. **3**, 385–390 (1998).

Vinogradov, G. V., A. Y. Malkin, and V. V. Volosevitch, V. P. Shatalov, and V. P. Yudin, "Flow, high-elastic (recoverable) deformations and rupture of uncured high molecular weight linear polymers in uniaxial extension," J. Polym. Sci., Polym. Phys. Ed. **13**, 1721–1735 (1975).

Walker, L. M., P. Moldenaers, and J.-F. Berret, "Macroscopic response of wormlike micelles to elongational flow," Langmuir **12**, 6309–6314 (1996).

Yao, M., G. H. McKinley, and B. Debbaut, "Extensional deformation, stress relaxation and necking failure of viscoelastic filaments," J. Non-Newtonian Fluid Mech. **79**, 469–501 (1998).

Yesilata, B., C. Clasen, and G. H. McKinley, "Nonlinear shear and extensional flow dynamics of wormlike surfactant solutions," J. Non-Newtonian Fluid Mech. **133**, 73–90 (2006).